

Wave-packet formation at the zero-dispersion point in the Gardner-Ostrovsky equation

A. J. Whitfield* and E. R. Johnson†

Department of Mathematics, University College London, London WC1E 6BT, United Kingdom

(Received 18 March 2015; published 18 May 2015)

The long-time effect of weak rotation on an internal solitary wave is the decay into inertia-gravity waves and the eventual emergence of a coherent, steadily propagating, nonlinear wave packet. There is currently no entirely satisfactory explanation as to why these wave packets form. Here the initial value problem is considered within the context of the Gardner-Ostrovsky, or rotation-modified extended Korteweg–de Vries, equation. The linear Gardner-Ostrovsky equation has maximum group velocity at a critical wave number, often called the zero-dispersion point. It is found here that a nonlinear splitting of the wave-number spectrum at the zero-dispersion point, where energy is shifted into the modulationally unstable regime of the Gardner-Ostrovsky equation, is responsible for the wave-packet formation. Numerical comparisons of the decay of a solitary wave in the Gardner-Ostrovsky equation and a derived nonlinear Schrödinger equation at the zero-dispersion point are used to confirm the spectral splitting.

DOI: [10.1103/PhysRevE.91.051201](https://doi.org/10.1103/PhysRevE.91.051201)

PACS number(s): 47.35.Fg, 92.10.Ei, 92.10.Hm, 42.65.–k

I. INTRODUCTION

The Korteweg–de Vries (KdV) equation is widely used to model oceanic internal waves, as described in the review by Helfrich and Melville [1]. In the KdV equation, a balance between the leading-order terms of weak nonlinearity and dispersion allows solitary-wave solutions. The wavelengths of these solitons decrease with increasing amplitude and fail to reproduce the broadening of the solitary waves that are often observed in oceanic waves at limiting amplitudes. To capture this broadening, a higher-order, cubic nonlinear term can be included [1]. This gives the extended KdV, or Gardner, equation,

$$\eta_t + \alpha_1 \eta \eta_x + \alpha_2 \eta^2 \eta_x + \beta_1 \eta_{xxx} = 0. \quad (1)$$

Here $\eta(x, t)$ is an interfacial displacement, and the coefficients α_1 , α_2 , and β_1 give the strengths of weak nonlinearity and weak nonhydrostatic dispersion.

Internal solitary waves can propagate for long distances over several inertial periods, potentially making the Earth's background rotational effects important. When rotational effects are significant, (1) is replaced by the Gardner-Ostrovsky (rotation-modified extended KdV) equation

$$(\eta_t + \alpha_1 \eta \eta_x + \alpha_2 \eta^2 \eta_x + \beta_1 \eta_{xxx})_x = \gamma \eta, \quad (2)$$

where background rotation has been introduced through the coefficient γ . For $\alpha_2 = 0$, Eq. (1) reduces to the KdV equation and (2) becomes the Ostrovsky equation; see Refs. [2,3]. Rotation removes the spectral gap in the Gardner equation required for the existence of solitary-wave solutions, and hence (2) predicts the complete decay of the otherwise persistent solitary wave into the inertia-gravity waves that have been introduced into the system by rotation [4,5]. This feature of rotational effects has recently received considerable attention. A combination of numerical simulations [6–9] and experiments [10] have all shown that not only does rotation cause a solitary wave to decay, but a nonlinear wave packet can eventually emerge from the radiation.

There appears to be no entirely satisfactory explanation for the emergence of these rotation-induced wave packets. Previous efforts have mainly focused on the near-linear limit of the Ostrovsky equation. For waves of wave number k , the linear Ostrovsky equation has a dispersion relation and group velocity

$$\omega_0 = \gamma/k - \beta_1 k^3 \quad \text{and} \quad c_g = -3\beta_1 k^2 - \gamma/k^2, \quad (3)$$

where $c_g = d\omega_0/dk$. The linear group velocity has a maximum at the finite nonzero wave number, $k_c = (\gamma/3\beta_1)^{-1/4}$, such that $d^2\omega_0/dk^2 = \omega_{0kk} = 0$.

Helfrich [6] observed that the nonlinear packets propagate at approximately the maximum linear group velocity. Grimshaw and Helfrich [7] subsequently formulated a theory based on this critical wave number k_c , although some of their numerical results disagreed with parts of their theory. Their theory also determined that the Ostrovsky equation is modulationally stable (defocusing) when the second-order dispersion coefficient is positive, $\omega_{0kk} > 0$, and unstable (focussing) when the second-order dispersion coefficient is negative, $\omega_{0kk} < 0$. Whitfield and Johnson [11] showed that the packets do not have a wave number precisely equal to k_c , nor do they travel exactly at the maximum linear velocity; instead, the packets have a wave number that is slightly larger than k_c and thus the packets lie in the modulationally unstable, $\omega_{0kk} < 0$, regime of the Ostrovsky equation.

The amplitude of the final emerging packet in Whitfield and Johnson [11] was accurately predicted as a function of the initial solitary-wave amplitude by the theory of Grimshaw and Helfrich [7], a prediction based on the assumption that only the energy from wave numbers near k_c , the zero-dispersion point where second-order dispersion vanishes, contributes to the formation of the packet. It has long been known in nonlinear optics that wave-packet solitons emerge from arbitrary initial pulses with central frequencies at the zero-dispersion point [12–14]. The soliton that emerges has a frequency shifted into the modulationally unstable regime, whereas the remaining energy from the initial pulse has frequency shifted into the stable regime. The process effectively divides the spectrum at the zero-dispersion point, leaving the energy shifted into the

*ashley.whitfield.12@ucl.ac.uk

†e.johnson@ucl.ac.uk

unstable regime to form a soliton and the energy shifted into the stable regime to disperse linearly to zero.

It is thus proposed here that a splitting of the spectrum at the zero-dispersion point, similar to that seen in nonlinear optics, could be the source of the observed rotation-induced wave packets. This is supported by integrations of the Gardner-Ostrovsky equation and a third-order nonlinear Schrödinger equation that considers only the initial disturbance energy near k_c .

II. THEORY

A. The Gardner-Ostrovsky equation

For oceanic internal solitary waves, it can be assumed without loss of generality that $\alpha_1, \beta_1, \gamma > 0$. The scaling, $x = L\tilde{x}$, $t = T\tilde{t}$, and $\eta = M\tilde{\eta}$ with $L^4 = \beta_1/\gamma$, $T = L^3/\beta_1$, and $M = \beta_1/\alpha_1 L^2$ [7], can thus be introduced to give a dimensionless Gardner-Ostrovsky equation,

$$(\tilde{\eta}_t + \tilde{\eta}\tilde{\eta}_x + \nu\tilde{\eta}^2\tilde{\eta}_x + \tilde{\eta}_{xxx})_x = \tilde{\eta}, \quad (4)$$

where only one parameter, $\nu = \alpha_2\sqrt{\gamma\beta_1}/\alpha_1^2$, remains. Equation (4) with “tildes” dropped will henceforth be referred to as the Gardner-Ostrovsky equation for $\nu \neq 0$ and the Ostrovsky equation for $\nu = 0$.

The Gardner equation has the soliton solution

$$\eta(\zeta) = a_s/[b + (1 - b)\cosh^2(\zeta/D)], \quad (5)$$

where $b = -a_s\nu/(2 + \nu a_s)$, $D^2 = 12/a_s(1 + \nu a_s/2)$, and $\zeta = x - st$ for $s = a_s(1 + \nu a_s/2)/3$. Setting $\nu = 0$ recovers the KdV equation sech^2 soliton solution. For $\nu < 0$, the Gardner soliton has the same polarity as the KdV soliton but broadens with increasing amplitude until a finite maximum amplitude $a_s = -1/\nu$ is reached. For $\nu > 0$, the Gardner soliton can have either polarity, but the broadening character is lost and the maximum amplitude criterion is replaced by a minimum amplitude $a_s = -2/\nu$ for $a_s\nu < 0$.

Small-amplitude evolutions, for initial conditions far from the wave-packet solution, closely follow linear Gardner-Ostrovsky equation dynamics [11], and so it is useful to consider the linear initial value problem. The solution of the linear Gardner-Ostrovsky equation with solitary-wave initial condition (5) (which is indeed far from the wave-packet solution) can be expressed as an inverse Fourier transform,

$$\eta(x, t) = \frac{1}{2\pi} \int_{-\infty}^{\infty} \hat{\eta}_0(k) \exp[ikx - i\omega_0(k)t] dk, \quad (6)$$

where $\hat{\eta}_0(k)$ is the Fourier transform of the initial condition (5). As the soliton (5) depends on ν , there are three different forms for $\hat{\eta}_0$,

$$\begin{aligned} \hat{\eta}_0(k) &= a_s\pi D \operatorname{cosech}(k\pi D/2) \\ &\times \begin{cases} b^{-1/2} \sin[kD \operatorname{arccosh}(b + 1/b - 1)/2] & (\nu < 0), \\ kD & (\nu = 0), \\ (-b)^{-1/2} \sinh[kD \operatorname{arccos}(1 + b/1 - b)/2] & (\nu > 0). \end{cases} \end{aligned} \quad (7)$$

Near the wavefront, the linear group velocity (3) has a maximum and $k \approx k_c$. The linear solution (6) can thus be approximated in terms of the Airy function Ai as

$$\eta(x, t) \approx \frac{2\hat{\eta}_0(k_c)}{(12t)^{1/3}} \text{Ai}\left(\frac{x - c_g(k_c)t}{(12t)^{1/3}}\right) \cos[k_c x - \omega_0(k)t]. \quad (8)$$

B. Nonlinear Schrödinger equation with third-order dispersion

To support the proposition that it is only the energy near the zero-dispersion point, $k = k_c$, that determines the form of the final wave packet, a nonlinear Schrödinger equation (NLS) is derived for a $k \approx k_c$ wave train in the Gardner-Ostrovsky equation. Grimshaw and Helfrich [7] derived an extended NLS for the Ostrovsky equation, and since the derivation here for the Gardner-Ostrovsky equation is similar, only a brief outline is given.

Consider a quasimonochromatic, small-amplitude wave train with an asymptotic expansion of the form

$$\eta(x, t) = A_0 + A \exp(i\theta) + \text{c.c.} + A_2 \exp(2i\theta) + \text{c.c.} + \dots, \quad (9)$$

where c.c. denotes the complex conjugate of the preceding term, $\theta = kx - \omega_0 t$, and $|A| \ll 1$. Assume also that $A(x, t)$ is slowly varying and $A_2 \sim O(|A|^2)$. Substituting (9) into (4) and following the method outlined in Ref. [7], it can be shown that $A_0 \sim O(|A|^4)$ and the leading-order term A satisfies the NLS,

$$i[A_t + c_g(k)A_x] + \frac{1}{2}\omega_{0kk}A_{xx} + \mu|A|^2A = 0, \quad (10)$$

with $\mu(k) = \mu_1 - \nu k$, and where $\mu_1(k) = -2k^3/(12k^4 + 3)$ is the NLS nonlinear coefficient for the Ostrovsky equation [7]. Equation (10) describes the evolution of a wave-train envelope $A(x, t)$ with wave number k in the weakly nonlinear limit of the Gardner-Ostrovsky equation. The presence of the Gardner term ν means that the nonlinear coefficient μ can take either sign—contrasting with the Ostrovsky equation, in which μ is always negative (as $\mu_1 < 0$). For ν sufficiently negative, the regions of modulational instability can switch: the Ostrovsky equation is focusing for waves with $k > k_c$ and defocusing for $k < k_c$, whereas if $\nu < \mu_1(k)/k$ the Gardner-Ostrovsky equation is focusing for $k < k_c$ and defocusing for $k > k_c$. In all cases, stable and unstable parts of the spectrum are divided at k_c .

When $k = k_c$, the second-order dispersion coefficient ω_{0kk} vanishes, and consequently this critical wave-number value is often referred to as the zero-dispersion point. Due to higher-order dispersive effects, dispersion at this point is not, however, identically zero. Rescaling brings in a third-order dispersion term to give the equation

$$i[A_t + c_g(k_c)A_x] - i\frac{1}{6}\omega_{0kkk}A_{xxx} + \mu|A|^2A = 0, \quad (11)$$

referred to here as the third-order NLS (TNLS [15]).

Unlike the NLS, the TNLS has no soliton solutions [12,16,17]. To model the Ostrovsky equation wave packets, Grimshaw and Helfrich [7] included some of the higher-order nonlinear terms and thus obtained analytical soliton solutions for an extended TNLS. These solitons, however, appeared to agree less well with the observed wave packets than did soliton solutions of the standard NLS with second-order dispersion [11].

A small-amplitude disturbance in the Gardner-Ostrovsky equation evolves according to (8). This corresponds to the form

$$A(x,t) \approx \frac{\hat{\eta}_0(k_c)}{(12t)^{1/3}} \text{Ai} \left(\frac{x - c_g(k_c)t}{(12t)^{1/3}} \right) \quad (12)$$

for the full TNLS, and it is the exact solution of the linear TNLS with initial condition

$$A(x,0) = \hat{\eta}_0(k_c)\delta(x). \quad (13)$$

This can be interpreted as stating that the initial condition for the TNLS is given by taking the energy at the zero-dispersion point in the given initial condition for the Gardner-Ostrovsky equation and regarding it as concentrated at the origin. The TNLS with this initial condition can be seen as a model for the leading waves in the small-amplitude limit of the rotation-induced decay of a solitary wave in the Gardner-Ostrovsky equation.

III. ANALYSIS AND NUMERICAL RESULTS

Section II proposed the TNLS as the evolution model for solitary-wave decay and subsequent wave-packet formation in the weakly nonlinear limit. It is also proposed that the shifting of energy at the zero-dispersion point into the unstable spectrum of the TNLS is the mechanism by which the rotation-induced packets form. To test these hypotheses, numerical integrations of corresponding initial value problems for the TNLS and Gardner-Ostrovsky equation were performed.

A spectral code with sponge regions at the domain edges was used to integrate both equations. The linear solution (12) was taken as the initial condition in all integrations of the TNLS. The starting time t_l for the linear solution was varied with a_s so that $a_s^2 t_l$ remained constant to ensure that the increasing nonlinearity of (11) was taken into account. For $a_s = 4$ and $\nu = -0.1, 0$, the starting time was taken as $t_l = 10$ and as $t_l = 2.5$ for $\nu = 0.1$ due to the more rapid onset of nonlinear effects. It was confirmed from higher-resolution computations that the evolutions did not differ from evolutions with smaller values of t_l .

Reference [11] showed that the decay of a solitary wave of amplitude $a_s = 4$ in the Ostrovsky equation was predominantly governed by the linear dynamics for times up to $t = 100$. It is therefore expected that the weakly nonlinear TNLS theory should apply at this amplitude of initial condition. Figure 1 shows a comparison at $t = 1000$ for integrations of the Ostrovsky equation [Fig. 1(a)] and TNLS [Fig. 1(b)]. The solutions are plotted in the frame moving at the maximum linear group velocity $c_g(k_c)$, and for comparison the TNLS solution, A , is plotted in the form $\eta = A \exp(i\theta) + \text{c.c.}$ [see Eq. (9)]. For the Ostrovsky equation integration, as expected, the solitary wave has decayed and a wave packet has emerged. The TNLS integration has also reproduced this decay and formation process. The packets produced by both equations have very similar amplitude and wavelengths, suggesting that not only is the TNLS capturing the mechanism by which the packets form, it is also correctly capturing the dynamics of the packet itself.

The wave-number spectra of the integrations from Fig. 1 are shown in Fig. 2, where the zero-dispersion point ($k = k_c$)

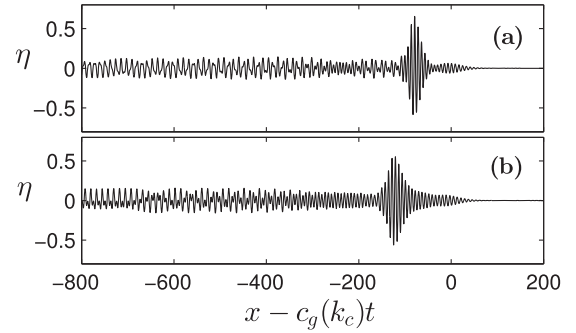


FIG. 1. Solutions at $t = 1000$ for integrations of the Ostrovsky equation (a) and TNLS (b). (a) A wave packet formed from the decay of a solitary wave of amplitude $a_s = 4$. (b) A wave packet formed from a δ function initial condition (13) with $a_s = 4$. The TNLS solution, A , is shown in the form $\eta = A \exp(i\theta) + \text{c.c.}$ [see Eq. (9)]. The solutions are remarkably similar even though (b) only models the evolution of the k_c wave numbers.

is represented by the vertical dashed line. The TNLS spectrum [Fig. 2(b)] has clearly split either side of the zero-dispersion point, as is expected, but importantly spectral splitting has also occurred in the Ostrovsky equation [Fig. 2(a)]. Spectral splitting at the zero-dispersion point is inevitable during the evolution of a weakly nonlinear pulse launched at the zero-dispersion point. In nonlinear optics, this phenomenon has previously been modeled using the TNLS [12–14]. The energy shifted into the modulationally unstable spectral space, where second-order dispersion dominates, forms a wave-packet soliton. As third-order dispersion is no longer dominant, the dynamics of the wave-packet soliton are then described by the standard NLS bright soliton wave-packet solution, explaining why Ref. [11] found that the standard NLS correctly predicted the packet shape and speed. Additionally, it is known that packet solitons produced in this manner have a wave number sufficiently close to the zero-dispersion point for third-order dispersion to act as a small perturbation in the standard NLS leading to exponentially small “tails” [12,16] (also found in Ref. [11]).

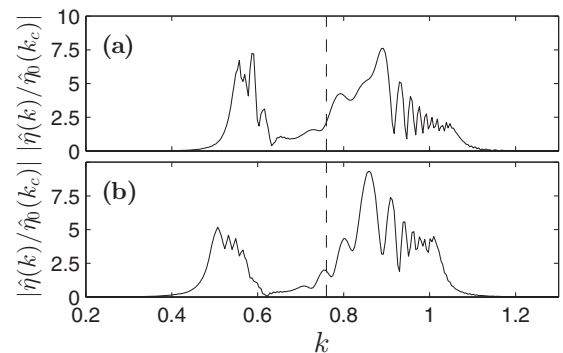


FIG. 2. Wave-number spectra at $t = 1000$ for integrations of the Ostrovsky equation (a) and TNLS (b). (a) The spectrum from the decay of a solitary wave of amplitude $a_s = 4$. (b) The spectrum from a δ function initial condition (13) with $a_s = 4$. The TNLS spectrum has been positively shifted by k_c to correspond to Fig. 1(b). The dashed line gives the wave number $k = k_c$.

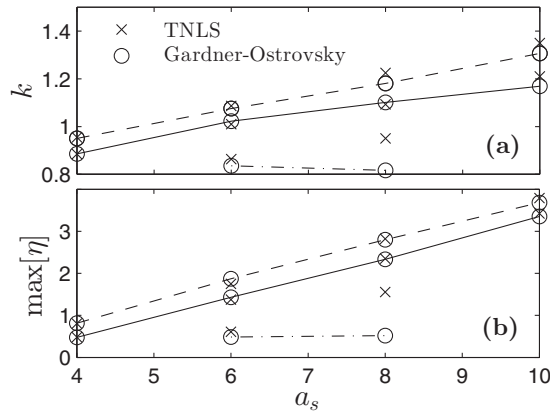


FIG. 3. Attributes of the wave packets at $t = 5000$ produced from integrations of the TNLS (crosses) and the Gardner-Ostrovsky equation (circles) simulating the rotation-induced decay of solitary waves with amplitude a_s . The solid, dashed, and dash-dotted lines show the integration results for Gardner term values $\nu = 0, 0.1$, and -0.1 , respectively. (a) The measured wave-packet wave number k . (b) The measured maximum wave-packet amplitude $\max[\eta]$.

The TNLS models the evolution of the energy contained in the initial solitary wave near the wave number k_c alone, yet Figs. 1(a), 1(b), 2(a), and 2(b) are remarkably alike. It appears that in the weakly nonlinear limit, all wave numbers other than those near k_c disperse away linearly with a negligible effect on packet formation. This supports the hypothesis that spectral splitting at the zero-dispersion point is the source of the wave packet that forms from the rotation-induced decay of a solitary wave.

To examine whether the observations above can be extended to the decay of larger-amplitude solitons, where the processes are not weakly nonlinear, and whether the results can be extended to the Gardner-Ostrovsky equation, a series of integrations for $\nu = 0, \pm 0.1$ were performed. For each value of ν , integrations for solitons of amplitude $a_s = 4, 6, 8$, and 10 were performed in both the Gardner-Ostrovsky equation and the corresponding TNLS initial value problem. The integrations were run until $t = 5000$ and then the wave number and maximum amplitude of the packets were measured. The wave number was found by measuring the largest peak in the Fourier transform. The results are summarized in Fig. 3. For the Ostrovsky equation ($\nu = 0$), the TNLS produces an almost identical packet wave number and amplitude even at $a_s = 10$. This trend is reproduced in the $\nu = 0.1$ results. However, for the Gardner-Ostrovsky integrations with $\nu = -0.1$, no wave packet at $a_s = 4$ or 10 was found by $t = 5000$. There is also significant disagreement for $a_s = 8$. This is to be expected. In the NLS model (10), the strength of nonlinearity is given by the coefficient $\mu = \mu_1 - \nu k$, where μ_1 is always negative. When the Gardner term ν is small and negative, it opposes the nonlinearity resulting from the Ostrovsky equation μ_1 , hence reducing the total nonlinearity of the problem. For $\mu \approx 0$, it is expected that, at least to a first-order approximation, the wave evolution will behave almost linearly. For the values under consideration here, $\nu = -0.1$ and $\mu \approx -0.05$, it is thus expected the nonlinear packets will take longer to form, which is exactly what is seen for $a_s = 4$ and 10 . The

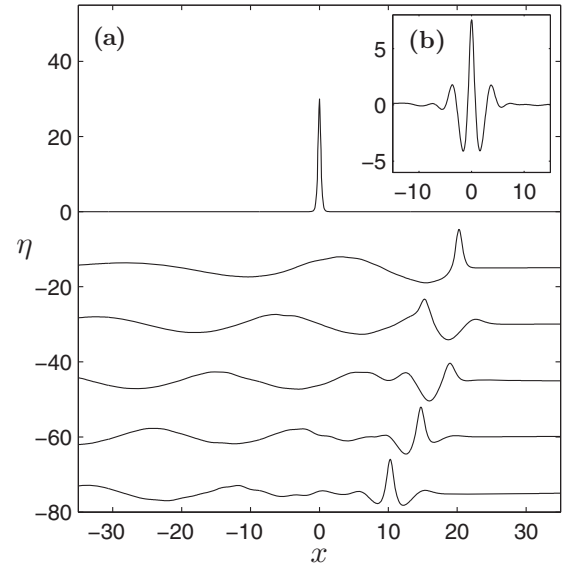


FIG. 4. Integration of the Gardner-Ostrovsky equation with $\nu = 0.2$ and solitary-wave initial condition of amplitude $a_s = 30$. The solution profile at times $t = 0, 1, 2, 3, 4, 5$ (a) and $t \approx 100$ (b). The initial condition contains the same energy at the zero-dispersion point, k_c , as the initial condition in Fig. 5. Note the similarity of the packet here to that of Fig. 5(b).

discrepancy at $a_s = 8$ is explained similarly since for $|\mu| \ll 1$, Eqs. (10) and (11) no longer represent the leading-order balance between nonlinearity and dispersion. In this case, higher-order nonlinear terms should be added to give an equation similar to that for the Ostrovsky equation in Ref. [7].

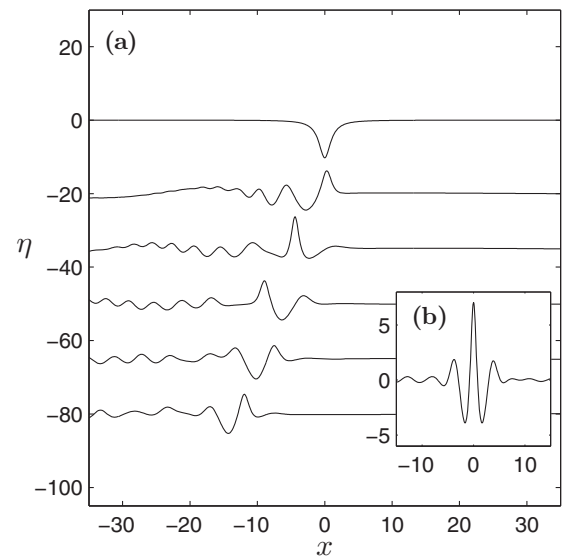


FIG. 5. Integration of the Gardner-Ostrovsky equation with $\nu = 0.2$ and solitary-wave initial condition of amplitude $a_s = -10.2303$. The solution profile at times $t = 0, 1, 2, 3, 4, 5$ (a) and $t \approx 100$ (b). The initial condition contains the same energy at the zero-dispersion point, k_c , as the initial condition in Fig. 4. Note the similarity of the packet here to that of Fig. 4(b).

If the hypotheses here are correct and the formation of rotation-induced packets can be described fully by the TNLS, then it follows that the only information in the initial solitary wave that determines the packet that eventually forms is the value of its Fourier transform at k_c , i.e., $\hat{\eta}_0(k_c)$. The Gardner solitons (5) include solitons with the same value of $\hat{\eta}_0(k_c)$ but distinctly different shapes and even opposite polarities. One strikingly contrasting example in which this occurs is when $\nu = 0.2$, so the Gardner equation has soliton solutions with amplitudes 30 and -10.2303 whose Fourier transform amplitudes at k_c are the same to four decimal places. Figures 4(a) and 5(a) show the temporal evolution for this example starting with the initial condition at the top. The resulting packets at $t \approx 100$ are shown in Figs. 4(b) and 5(b). The initial conditions differ greatly, as do their subsequent evolutions until the wave packet forms. Nevertheless, comparing Figs. 4(b) and 5(b) suggests that the fully formed packets for the integrations are almost identical, as predicted by the zero-dispersion theory, supporting the hypothesis that for a given initial condition it is the energy in the spectrum at the zero-dispersion point, k_c , alone that determines the characteristics of the wave packet that forms.

IV. CONCLUSION

The long-time outcome of the decay of a solitary wave due to rotational effects is the formation of a nonlinear wave packet. Here this problem has been considered within the framework of the Gardner-Ostrovsky equation, which has a maximum linear group velocity at the finite nonzero wave number k_c , referred to as the zero-dispersion point because second-order dispersion vanishes there. It has been hypothesized here that, in the evolution of an initial solitary wave, energy from all wave numbers except those near k_c disperses linearly, leaving only the energy near k_c to form a wave packet. It follows that the evolution should be closely described by a third-order nonlinear Schrödinger equation (TNLS) centered on k_c . These hypotheses were supported by comparing numerical integrations of the TNLS with numerical integrations of the full Gardner-Ostrovsky equation, and they were further supported by two integrations of the Gardner-Ostrovsky equation with markedly different initial conditions (including opposite

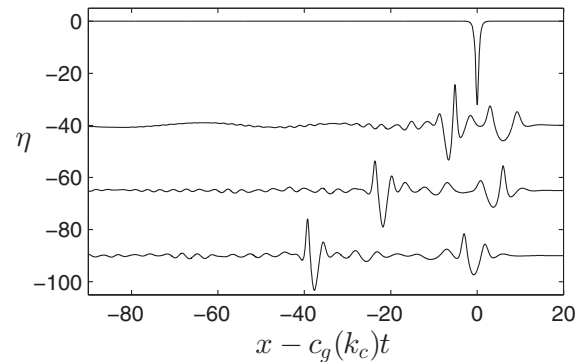


FIG. 6. Integration of the Gardner-Ostrovsky equation with $\nu = 0.1$ and solitary-wave initial condition of amplitude $a_s = -32$. The solution profile is shown at times $t = 0, 2.5, 7.5, 12.5$. Two persistent wave packets emerge.

parity) but the same initial energy at k_c , which each produced the same wave packet. The zero-dispersion point divides the spectrum of the Gardner-Ostrovsky equation into regions that are either modulationally stable or modulationally unstable. It was proposed that the initial energy near the zero-dispersion point splits, and it is the energy shifted into the unstable region that forms the wave packet. This was supported by computations of the wave-number spectra for evolutions of the Gardner-Ostrovsky equation and TNLS.

The soliton amplitudes considered in Figs. 4(a) and 5(a) are large with predominantly nonlinear dynamics, yet the zero-dispersion point theory correctly predicted that the resulting packets [Figs. 4(b) and 5(b)] would be the same. This suggests that the zero-dispersion point theory could perhaps apply outside of the weakly nonlinear regime where the NLS analysis is valid.

To date, studies have shown only a single packet forming from the decay of an initial solitary wave. This is not a requirement for the analysis here, and it is possible that if sufficient energy is shifted into the unstable region of the spectrum, more than one wave packet could form. Figure 6 shows that this does in fact occur, giving an evolution in which two packets form from a single solitary wave.

-
- [1] K. R. Helfrich and W. K. Melville, *Annu. Rev. Fluid Mech.* **38**, 395 (2006).
 - [2] L. A. Ostrovsky, *Oceanology* **18**(2), 119 (1978).
 - [3] R. Grimshaw, *Stud. Appl. Math.* **73**, 1 (1985).
 - [4] R. H. J. Grimshaw, J.-M. He, and L. A. Ostrovsky, *Stud. Appl. Math.* **101**, 197 (1998).
 - [5] R. H. J. Grimshaw and K. R. Helfrich, *IMA J. Appl. Math.* **77**, 326 (2012).
 - [6] K. R. Helfrich, *Phys. Fluids* **19**, 026601 (2007).
 - [7] R. H. J. Grimshaw and K. R. Helfrich, *Stud. Appl. Math.* **121**, 71 (2008).
 - [8] M. Stastna, F. J. Poulin, K. L. Rowe, and C. Subich, *Phys. Fluids* **21**, 106604 (2009).
 - [9] K. R. Khusnutdinova and K. R. Moore, *Wave Motion* **48**, 738 (2011).
 - [10] R. H. J. Grimshaw, K. R. Helfrich, and E. R. Johnson, *Phys. Fluids* **25**, 056602 (2013).
 - [11] A. Whitfield and E. Johnson, *Phys. Fluids* **26**, 056606 (2014).
 - [12] P. K. A. Wai, H. H. Chen, and Y. C. Lee, *Phys. Rev. A* **41**, 426 (1990).
 - [13] M. Desaix, D. Anderson, and M. Lisak, *Opt. Lett.* **15**, 18 (1990).
 - [14] P. Wai, C. Menyuk, H. Chen, and Y. Lee, *Opt. Lett.* **12**, 628 (1987).
 - [15] J. Yang and T. Akylas, *Stud. Appl. Math.* **111**, 359 (2003).
 - [16] R. Grimshaw, *Stud. Appl. Math.* **94**, 257 (1995).
 - [17] V. Zakharov and E. Kuznetsov, *J. Exp. Theor. Phys.* **86**, 1035 (1998).